

國立交通大學

電機資訊學院
光電工程研究所

博士論文

液晶薄膜場致轉向動態之時析振動光譜研究

Multichannel Time-Resolved Vibrational
Spectroscopy of the Field-Induced Reorientation
Dynamics of Liquid Crystal Thin Films



研究生：施文慈

指導教授：黃中堯 教授

中華民國九十四年七月

液晶薄膜場致轉向動態之時析振動光譜研究
Multichannel Time-Resolved Vibrational Spectroscopy of
the Field-Induced Reorientation Dynamics of
Liquid Crystal Thin Films

研究生：施文慈

Student: Wen-Tse Shih

指導教授：黃中堯 教授

Advisors: Prof. Jung Y. Huang

國立交通大學電機資訊學院
光電工程研究所

博士論文

A Dissertation Submitted to
Department of Photonics and Institute of Electro-optical Engineering
College of Electrical Engineering and Computer Science
National Chiao Tung University
in Partial Fulfillment of the Requirements
for the Degree of
Doctor of Philosophy
in
Electro-optical Engineering

July 2005

Hsinchu, Taiwan, Republic of China

中華民國九十四年七月

國立交通大學

論文口試委員會審定書

本校光電工程研究所博士班 施文慈 君

所提論文 液晶薄膜場致轉向動態之時析振動光譜研究

合於博士資格標準、業經本委員會評審認可。

口試委員：張景園

張景園 教授

趙如蘋

趙如蘋 教授

黃華宗

黃華宗 教授

吳俊傑

吳俊傑 教授

林宏洲

林宏洲 教授

指導教授：黃中堯

黃中堯 教授

所長：賴映杰 教授

系主任：馮厚靈 教授

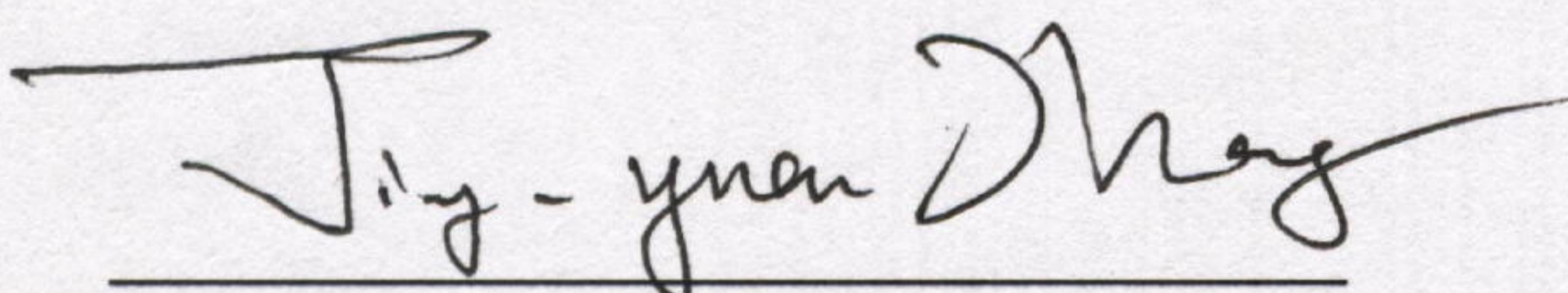
中華民國 94 年 7 月 27 日

Institute of Electro-Optical Engineering
National Chiao Tung University
Hsinchu, Taiwan, R.O.C.

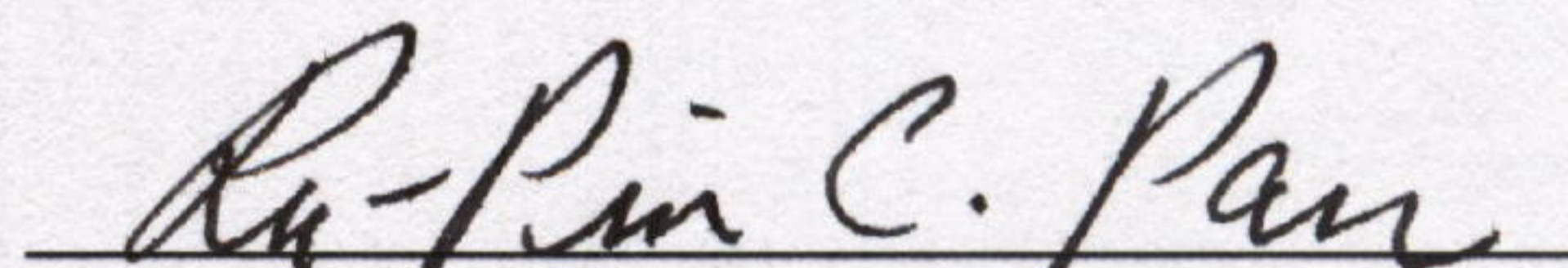
Date : July 27, 2005

We have carefully read the dissertation entitled Multichannel time-resolved vibrational spectroscopy of the field-induced reorientation dynamics of liquid crystal thin films

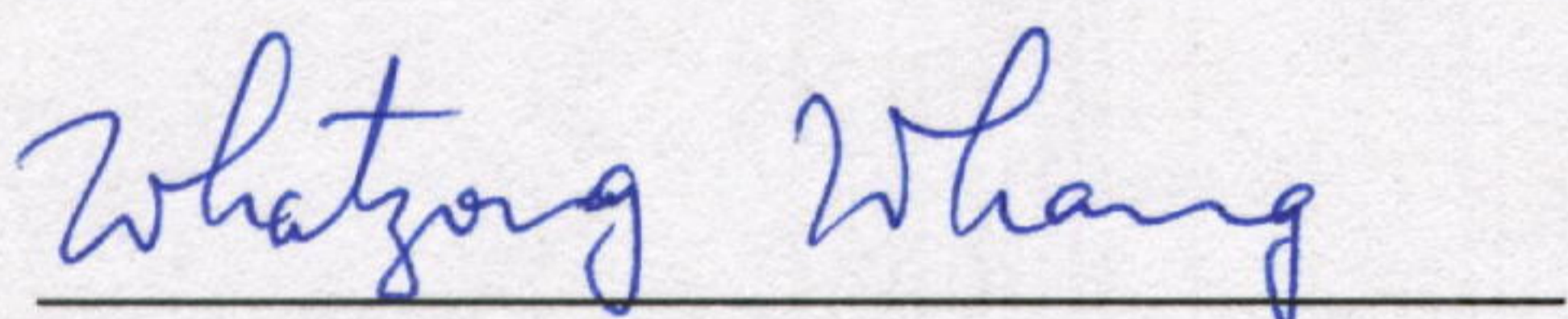
submitted by Wen-Tse Shih in partial fulfillment of the requirements of the degree of DOCTOR OF PHILOSOPHY and recommend its acceptance.



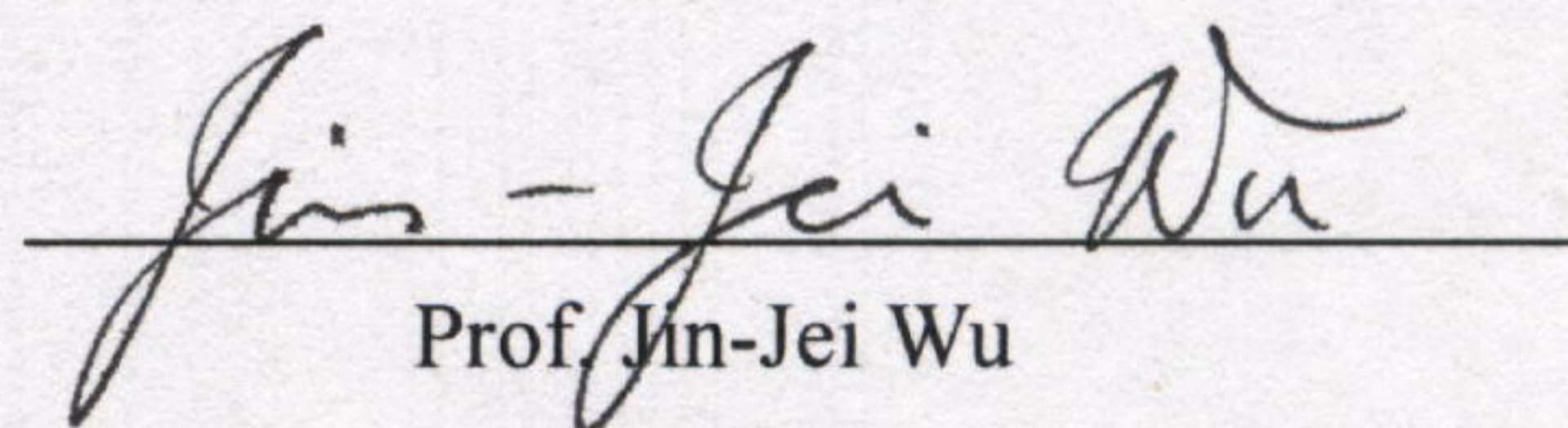
Prof. Jing-Yuan Zhang



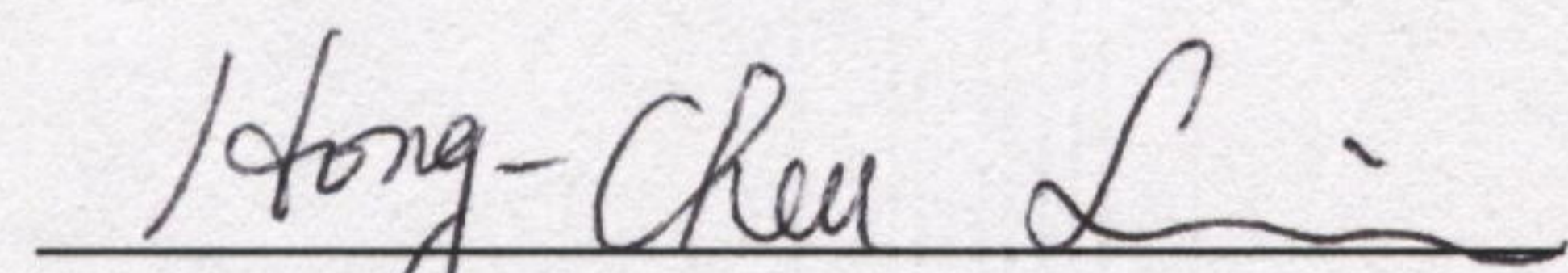
Prof. Ru-Pin Chao Pan



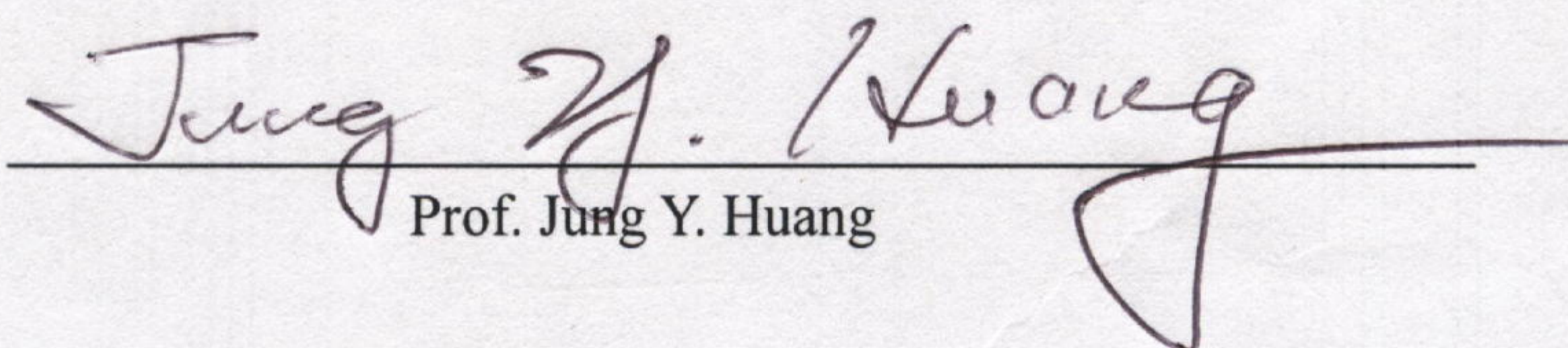
Prof. Wha-Tzong Whang



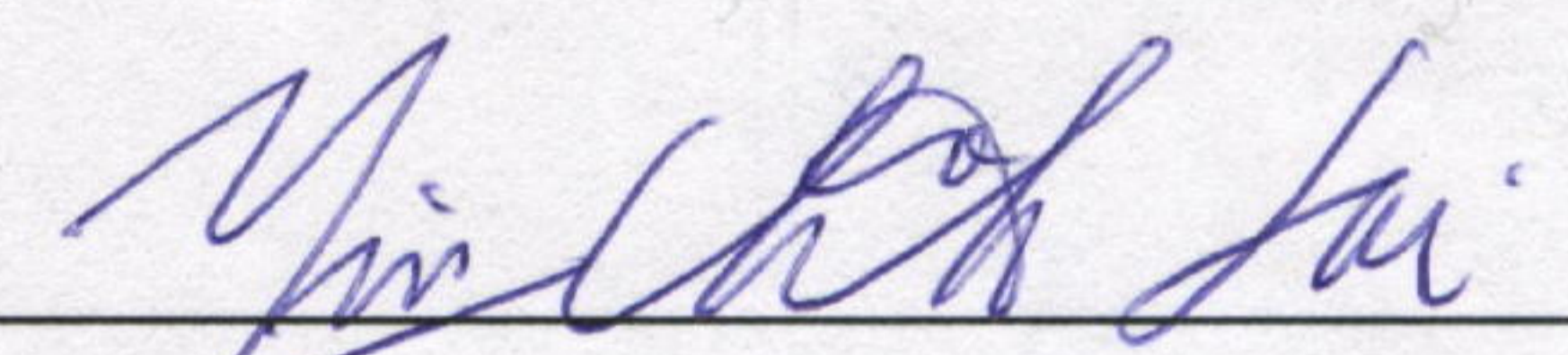
Prof. Jin-Jei Wu

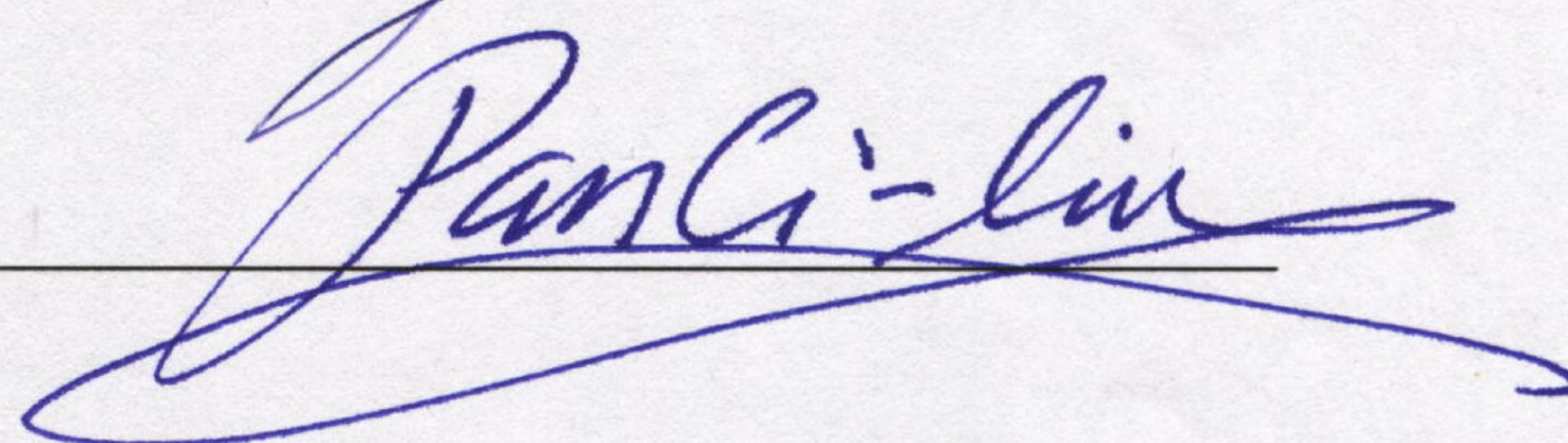


Prof. Hong-Chou Lin

Thesis Advisor : 

Prof. Jung Y. Huang

Director of Institute of Electro-Optical Engineering : 

Chairman of Department of Photonics : 

液晶薄膜場致轉向動態之時析振動光譜研究

研究生：施文慈

指導教授：黃中堯博士

國立交通大學

光電工程研究所

摘要

不論是在液晶物理的研究上，或是在液晶元件的發展上，場致分子轉向的動態過程都是一個重要課題。本論文利用偏振傅立葉轉換紅外光譜及拉曼光譜，研究向列反向扭轉液晶及表面穩定鐵電性液晶的場致分子轉向動態過程。在紅外吸收光譜量測方面，我們建構了一套多頻道時析系統進行高效率的動態光譜量測，並應用二維相關光譜技術分析量測的結果。對於二維相關光譜分析與異向性液晶薄膜的分子官能基排列及轉向之間的關連，也做了理論的模擬與討論。

由向列反向扭轉液晶的研究發現，液晶分子在沿著分子長軸方向會發生侷限性的旋轉，電光反應之亮度上升和下降時間分別是6和1.6毫秒，場致轉向的動態過程中液晶分子的運動並非剛體旋轉。

在表面穩定鐵電性液晶方面，我們觀察了鐵電性液晶純材料CMHCB在結晶相和鐵電相的分子構形及排列。二維相關光譜分析的結果反映出鐵電相中存在的Goldstone mode，而溫度變化引起的重新排列與分子官能基有關。場致轉向的過程始於分子內的運動，這個過程持續約不到10微秒。此外也發現CMHCB對於電場極性的反應並不對稱，這也表示在分子尺度中，相對於分子主軸的順時針與逆時針對稱性並不存在。

我們也研究了另一個鐵電性混合材料的場致轉向過程。從二維相關光譜分析結果可以看出，外加電場會抑制Goldstone mode。與前述的鐵電性純材料

相類似，此一表面穩定鐵電性混合材料的樣品對於電場的極性反應也不對稱，同樣在分子尺度中，相對於分子主軸的順時針與逆時針對稱性並不存在。瞬態過程中，場致分子轉向始於分子內部的運動，此一過程約持續10微秒，之後分子內部運動由單一分子座標內的官能基，傳遞到其他分子座標內的官能基。而分子官能基如C-O-C，C=C，及C-H均沿著傾斜的角錐面，以不同角度做相關但非一致性的旋轉。

本論文的研究結合了多頻道時析系統的分子振動光譜量測與二維相關光譜分析技術，這樣的方法對於場致動態分子形變、分子排列、次分子動力學以及分子與環境交互作用等相關研究，能夠有效率的觀測分析大量訊息，確實是個非常有用的方法。



Multichannel Time-Resolved Vibrational Spectroscopy of the Field-Induced Reorientation Dynamics of Liquid Crystal Thin Films

Student: Wen-Tse Shih

Advisors: Dr. Jung Y. Huang

Department of Photonics and Institute of Electro-optical Engineering,
National Chiao Tung University

Abstract

The field-induced molecular reorientation dynamics of a nematic twisted pi-cell and surface stabilized ferroelectric liquid crystals (SSFLC) had been studied with time-resolved polarized Fourier transform infrared spectroscopy (FTIR) and Raman spectroscopy. We constructed a multichannel time resolving system to perform the FTIR measurements and employed two dimensional (2D) correlation techniques to analyze the obtained IR spectra. The different information obtained from the 2D correlation technique and 2D hetero correlation technique was elucidated. The effects of the alignments and orientations of functional groups in an anisotropic film on the 2D correlation were also discussed.

The alignment of the LC molecules in a nematic twisted pi-cell was revealed. The results suggest that the molecules undergo a restricted rotation about the molecular long axis. The rise and decay times of the electro-optical response were found to be 6 ms and 1.6 ms, respectively. In the switching dynamic process, the LC molecules in the twisted pi-cell do not rotate like a rigid molecule during the field induced reorientation process.

A neat ferroelectric liquid crystal CMHCB in an SSFLC cell was studied. The molecular conformations and alignments of CMHCB in the K phase and SmC* phase were studied. The 2D IR correlations clearly exhibit Goldstone mode in the SmC* phase. The phase transition-induced re-arrangement was found to be

dependent on the molecular fragments. We demonstrated that the 2D IR correlation technique can reveal the field-induced collective reorientation of the molecular segments in the CMHCB. The reorientation process starts from the chiral part with an intramolecular motion, which proceeds in less than 10 μ sec. In addition, we found an asymmetry in the response of the CMHCB to electric field polarities, indicating that the clockwise–anticlockwise symmetry about the cone axis is broken.

The molecular motion of an SSFLC mixture during a field-induced reorientation process was studied. The 2D IR correlation technique clearly reveals that the thermal fluctuations in the azimuthal angle of the FLC director about a tilt cone in the SmC* phase with unwound structure are suppressed by an applied electric field. In addition, an asymmetry in the response of the surface stabilized FLC mixture to positive and negative driving pulses was also revealed in the 2D IR correlation analysis, indicating that similar to CMHCB, the clockwise–anticlockwise symmetry about the cone axis is broken at the molecular level in the FLC mixture. In a transient situation, the field-induced reorientation process was found to start with an intramolecular motion, which proceeds in about 10 μ sec. The intramolecular motion then propagates from the fragments attached to a single molecule to the ones belonging to different molecular coordinates. The molecular segments of C–O–C, C=C, and C–H stretch modes were found to rotate about a tilted cone with different angular speeds in a correlated but non rigid way.

The combination of multichannel time-resolved vibrational spectroscopy and 2D correlation spectroscopy demonstrated in this thesis shall be useful for the studies of field-induced transient molecular deformations and alignment, submolecular dynamics and molecular-environment interactions.

Contents

Abstract (in Chinese)	i
Abstract (in English)	iii
Contents	v
List of Tables	ix
List of Figures	x
1 Introduction	1
2 Pi cell and Surface Stabilized Ferroelectric Liquid Crystals	5
2.1 Liquid Crystals	5
2.1.1 Liquid Crystal Phases.	5
2.1.2 Chirality in Liquid Crystals	7
2.1.3 Basic Optics of a Liquid Crystal Thin Film	10
2.2 Liquid Crystal Display Technologies and Nematic Liquid Crystal Twisted Pi-Cell	12
2.2.1 LCD Technology Today	12
2.2.2 Nematic Twisted Pi-Cell	14
2.3 Surface Stabilized Ferroelectric Liquid Crystals	15
2.3.1 The SSFLC Structure	16
2.3.2 Polar Switching	17
2.4 Molecular Reorientation Dynamics of Liquid Crystal Thin Films	20

3	Time-Resolved Vibrational Spectroscopy	23
3.1	Infrared and Raman Spectroscopy	24
3.2	Time-Resolved FTIR	28
3.2.1	Principle of Asynchronous Time-Resolved FTIR Spectroscopy . . .	30
3.3	Multichannel Time-Resolved FTIR	36
3.3.1	Descriptions of the Multichannel Time-Resolved System	37
3.3.2	Accuracy Test of the Multichannel Time-Resolved System	39
3.4	Two-Dimensional Correlation Spectroscopy	41
3.4.1	Principle of Two-Dimensional Correlation Analysis	43
3.4.2	Properties of 2D Correlation Spectra.	44
4	Switching Dynamics of Twisted Nematic Liquid Crystal Pi-Cells	47
4.1	Experimental Procedures	47
4.2	Results and Discussion	50
4.2.1	Polarized Fourier-Transform Infrared Absorption Spectroscopy of a Twisted LC Pi-Cell	50
4.2.2	Raman Scattering Spectroscopy of Twisted LC Pi-Cells	56
4.2.3	Field-Induced Reorientation of Liquid Crystal Molecules in a Twisted Nematic Pi-Cell	58
4.3	Summary	61
5	Switching Dynamics of a Surface Stabilized Ferroelectric Liquid Crystal Mixture	62
5.1	Experimental Procedures	63
5.2	Second Harmonic Generation and Polarized FTIR Absorption Spectroscopy of an SSFLC	64
5.3	Results and Discussion	67
5.3.1	Steady-State Properties of an SSFLC	67
5.3.2	Field-Induced Reorientation	73
5.4	Summary	78

6	2D IR Correlation Spectroscopy of a Neat Surface Stabilized Ferroelectric Liquid Crystal	79
6.1	Experimental Procedures	80
6.2	Theoretical Considerations	81
6.2.1	Absorbance Profiles of Polarized IR Spectra	81
6.2.2	Theory of 2D IR Correlation	82
6.2.3	Determination of Molecular Configuration with 2D Correlation Analysis	83
6.2.3.1	Analyzing the Spectra at Same t	83
6.2.3.2	Analyzing the Spectra at Different t	86
6.3	Results and Discussion	87
6.3.1	Assignment of Infrared Absorption Bands	87
6.3.2	Polarized FTIR Spectra in the K Phase and SmC* Phase	89
6.3.3	Time-Resolved 2D IR Correlation Analysis	94
6.4	Summary	99
7	2D IR Correlation Spectroscopy of an Electro-Optical Switching Ferroelectric Liquid Crystal Mixture	101
7.1	Experimental Procedures	101
7.2	Results and Discussion	102
7.2.1	Assignment of Infrared Absorption Bands.	102
7.2.2	Time-Resolved Polarized FTIR Spectra	103
7.2.3	2D Polarized IR Correlation Analysis of the FLC Mixture in Steady State	107
7.2.4	Time-Resolved 2D IR Correlation Analysis of the Switching Dynamics of the FLC Mixture	109
7.3	Summary.	115
8	Conclusion and Future Prospect	116

Bibliography	119
Appendix Sample Preparations	125
I. Sample Substrate Cleaning Procedure.....	125
II. Alignment Layer Preparation.....	126
III. Cell Assembly and Liquid Crystal Filling.....	127



List of Tables

- 4.1. Calculated and measured normal- mode frequencies of cyano biphenyl51
- 5.1. Dichroic ratio D of infrared absorption peaks and angular shift $\Delta\Phi$ of azimuthal patterns with a steady dc field of opposite polarity. 71



List of Figures

2.1.	Molecular arrangement in the nematic, SmA and SmC phases.	6
2.2	Twist of the molecule in N* phase	8
2.3	Twist of the director in the SmC* phase	9
2.4	A typical setup for measuring the transmission intensity of a LC cell	11
2.5	Structure of a liquid crystal cell	15
2.6	A typical twisted pi-cell.	15
2.7	The basic geometry of an SSFLC cell structure applied with external electric fields	16
2.8	Schematics of a bookshelf structure with inclined layers and a chevron structure	17
2.9	Simplified model of the C* cone at the surface boundary in a cell with smectic layers tilted at angle δ	18
3.1	The excitation of a vibrational state in the electronic ground state S_0 by infrared absorption and Raman scattering.	26
3.2	Schematic of FTIR system	29
3.3	A typical setup for the asynchronous time-resolved measurement	30
3.4	The shapes of the signals in processes A-H in Fig. 3.3	33
3.5	Role of the low-pass filter	35
3.6	The schematics of the data acquisition procedure of the time-resolved measurement	37
3.7	Schematic diagram of a multichannel FTIR system	38
3.8	Comparison of the interferograms of air obtained from the MCFTIR system and the conventional FTIR spectrometer	40
3.9	The interferograms of air obtained from the 32 channels in the multichannel time-resolved system	40

3.10	General scheme for obtaining 2D correlation spectra	42
3.11	Schematic contour map of a synchronous 2D correlation spectrum and an asynchronous 2D correlation spectrum	45
4.1	Measured optical transmission of a twisted pi-cell as a function of applied voltage	48
4.2	Experimental setup for acquiring transient Raman spectra from a LC cell during the field-induced switching process	49
4.3	Fourier-transform infrared absorption spectrum of a twisted pi-cell with an applied voltage of 0 V	50
4.4	Azimuthal patterns of the infrared absorption peaks of a twisted pi-cell with varying applied voltages	52
4.5	Schematic diagram showing the relationship between the molecular frame ($\xi\eta\zeta$) and the laboratory coordinates system (XYZ)	53
4.6	The infrared dichroic ratio and the intensity ratio of the infrared absorption peaks plotted as a function of voltage	55
4.7	Raman spectra from a twisted pi-cell with varying applied voltage	56
4.8	Raman spectra near the C–H stretching region from a twisted pi-cell with varying applied voltages	57
4.9	Normalized Raman peak intensities versus applied voltage	58
4.10	Optical transmission through a twisted pi-cell lying between a set of crossed polarizer and analyzer	59
4.11	Raman spectra from a twisted pi-cell at varying time	60
4.12	Normalized Raman peak intensities versus time	60
5.1	Schematic diagram showing the relationship among the molecular frame ($\xi\eta\zeta$), layer frame ($X_1Y_1Z_1$) and laboratory coordinates system (XYZ)	65
5.2	Theoretical curves of the azimuthal FTIR patterns with IR dipole moment pointing to $\beta = 0^\circ$ or $\beta = 90^\circ$ of an SSFLC	66
5.3	Theoretical curves of azimuthal patterns of second harmonic generation for an SSFLC cell with various optical beam polarization combinations	67

5.4	FTIR spectra of an SSFLC measured without applied electric field	68
5.5	Normalized IR azimuthal patterns of various atomic groups associated with the FLC core and the alkyl chains and C–O moiety	70
5.6	Azimuthal patterns of the second harmonic generation signal from an SSFLC with various polarization combinations	72
5.7	The p-polarized second harmonic signal from an SSFLC cell excited by a p-polarized fundamental beam.	72
5.8	Electro-optical azimuthal patterns measured on an SSFLC during the field-on and field-free durations.	74
5.9	The dynamic variations of fitting parameters of the electro-optical azimuthal patterns and the applied voltage, and the deduced orientation angle of the optic axis of the SSFLC	75
5.10	Time-resolved FTIR spectra taken from an SSFLC, which is excited by +10 V pulse extending from 0 to 110 μ sec.	75
5.11	Transient orientations of several atomic segments associated with the FLC cores are presented as a function of delay time.	77
5.12	Transient orientations of several atomic segments associated with C=O moiety and alkyl chain are presented as a function of delay time	77
6.1	Structure of CMHCB and the phase transition temperature	81
6.2	The influence of the isotropic term A_0 on 2D IR correlation.	84
6.3	The influence of the uniaxial component U on 2D IR correlation	85
6.4	The influence of the orientation Φ_0 of molecular fragment on the 2D IR correlations	86
6.5	Infrared absorption spectrum of an SSFLC cell of CMHCB in SmC* at 108 °C and a set of polarized IR spectra for the SSFLC cell at 108 °C and zero field	87
6.6	Synchronous and asynchronous 2D IR correlation plots in the 1720–1780 cm^{-1} region generated from the polarization-angle dependent spectra of CMHCB at 108 °C in the field-free virgin state	88

6.7	The azimuthal absorbance profiles of IR peaks at 1604, 1261, 2974, and 1161 cm^{-1} at 65 °C and 108 °C in the field-free virgin state.	90
6.8	The schematic illustration of molecular orientation in the SmC* and K phases	91
6.9	Synchronous 2D IR correlation plot in the field-free virgin state generated from the polarization-angle dependent spectra of CMHCB at 65 °C and 108 °C	92
6.10	Asynchronous 2D IR correlation plot in the field-free virgin state generated from the polarization-angle dependent spectra of CMHCB at 65 °C and 108 °C	92
6.11	Asynchronous 2D IR hetero correlation plot in the field-free virgin state generated from the polarization-angle dependent spectra of CMHCB between at 65 °C and at 108 °C	93
6.12	Comparison of the dichroic ratios and the 2D IR synchronous auto peak, and the comparison of the apparent angles and the 2D IR hetero asynchronous auto peak of C=C stretching mode	95
6.13	Dynamic variations of the hetero asynchronous correlation and the averaged hetero asynchronous correlation of C=C and C–O–C stretching modes	97
6.14	Dynamic variations of the 2D IR synchronous correlation and the hetero asynchronous correlation of C=O stretching modes	98
6.15	Time derivatives of the dynamic variations of the 2D IR hetero asynchronous correlation in the positive-voltage driving cycle and negative-voltage driving cycle	99
7.1	Infrared absorption spectrum and a set of polarized IR spectra of an SSFLC cell of FELIX 017/100 in SmC* at 35 °C in the field-free state	103
7.2	The electro-optical response and the average apparent angles of selected IR absorption peaks and the time courses of the dichroic ratios of the C=C stretch mode and C–O–C stretch	105

7.3	Comparison of the dichroic ratios and the 2D IR synchronous auto peak of C–O–C stretch at 1252 cm ⁻¹ and C=C stretch mode at 1608 cm ⁻¹	106
7.4	Synchronous and asynchronous 2D IR correlation spectrum generated from the polarized spectral variations of FELIX 017/100 at 35°C without an external field, applying dc +5 V and -5 V	108
7.5	Time courses of 2D IR hetero asynchronous auto peaks generated from the time-resolved polarization-angle dependent spectra of FELIX 017/100 at 35 °C	110
7.6	Time derivatives of the dynamic variations of the 2D IR asynchronous hetero correlation in positive-voltage and negative-voltage driving cycles	111
7.7	Dynamic variations of the 2D IR asynchronous correlation of C=C stretching modes and C–O–C stretching modes with respect to the C=C stretching mode at 1609 cm ⁻¹	112
7.8	Dynamic variation of the angular spread of the functional groups associated with the core segments relative to that along to the C=C stretching mode	113
7.9	The time courses of 2D IR synchronous auto peaks generated from the time-resolved polarization-angle dependent spectra from 0° to 180° of FELIX 017/100 at 35 °C	114